





LETTER OPEN



ACUTE LYMPHOBLASTIC LEUKEMIA

UBTF::ATXN7L3 gene fusion defines novel B cell precursor ALL subtype with CDX2 expression and need for intensified treatment

Lorenz Bastian ^{1,2,3}, Alina M. Hartmann^{1,2,3}, Thomas Beder^{1,2,3}, Sonja Hänzelmann^{1,2,3}, Jan Kässens ^{1,2}, Miriam Bultmann^{1,2}, Marc P. Hoepfner^{3,4}, Sören Franzenburg⁴, Michael Wittig⁴, Andre Franke⁴, Inga Nagel⁵, Malte Spielmann^{5,6}, Niklas Reimer ^{2,7,8}, Hauke Busch ^{2,7,8}, Stefan Schwartz⁹, Björn Steffen¹⁰, Andreas Viardot¹¹, Konstanze Döhner¹¹, Mustafa Kondakci¹², Gerald Wulf¹³, Knut Wendelin¹⁴, Andrea Renzelmann¹⁵, Alexander Kiani ^{16,17}, Heiko Trautmann^{1,2}, Martin Neumann^{1,2,3}, Nicola Gökbüget¹⁰, Monika Brüggemann^{1,2,3} and Claudia D. Baldus ^{1,2,3} ✉

© The Author(s) 2022

Leukemia (2022) 36:1676–1680; <https://doi.org/10.1038/s41375-022-01557-6>

TO THE EDITOR:

Genomic aberrations—gene fusions in the majority of cases—and corresponding transcriptional regulations define an increasingly complex landscape of molecular subtypes in B cell precursor acute lymphoblastic leukemia (BCP-ALL) [1]. Up to 15% of patients cannot be allocated to established subtypes, suggesting the presence of unrecognized drivers—especially in adult patients who have been less studied so far.

We performed transcriptome sequencing (RNA-Seq) on $n = 568$ adult BCP-ALL patients prospectively treated according to pediatric-based protocols of the German Multicenter Acute Lymphoblastic Leukemia (GMALL) study group including risk stratification based on minimal residual disease (MRD) and treatment intensification for high-risk patients. To define molecular subtypes, we used our previous integrative analyses [1] to train a machine learning classifier to predict subtype allocation from gene expression profiles of subsequently sequenced samples. Feature selection (LASSO) was used to identify the most informative genes. Underlying genomic aberrations were analyzed (whole-genome sequencing (WGS), whole-exome sequencing (WES); SNP-arrays) to confirm subtype allocation in selected cases. With this approach, we were able to allocate $n = 535/568$ (94%) samples to 15 previously established [1] molecular subtypes (Fig. 1A–D), with confirmation of corresponding genomic alterations in 91% of analyzed cases (Fig. 1D). Unsupervised gene

expression analysis of previously unassigned samples revealed a distinct patient subset ($n = 12$; Supplementary Fig. S1A) defined by a novel in-frame gene fusion of upstream binding transcription factor (*UBTF*) and ataxin-7-like protein 3 (*ATXN7L3*) occurring exclusively in this patient cluster ($n = 12/12$ vs. $n = 0/556$ in remaining cohort, $p < 1E-10$; Fig. 1D). Comparison of gene expression profiles revealed that *UBTF::ATXN7L3* rearranged cases in our cohort match to a recently described BCP-ALL subtype, which so far was identified by increased expression of the homeobox transcription factor CDX2 ('CDX2 high' ALL) [2] (Supplementary Fig. S1B). *UBTF::ATXN7L3* represents an 11.3 kbp in-frame read-through between *UBTF* exon 17/21 and a 5' UTR splice site of *ATXN7L3*, with the same sanger sequencing confirmed break point in all samples (Fig. 2A, Supplementary Methods). WGS of 3 samples revealed a 10.08 kb genomic deletion involving *UBTF* 3' exons (18–21) and most of the intergenic region between *UBTF* and *ATXN7L3* as underlying mechanism (Fig. 2A, Supplementary Fig. S2). Break-point-specific PCR and Sanger sequencing confirmed presence of the deletion in $n = 11/11$ *UBTF::ATXN7L3* patients with available material (Supplementary Fig. S3). The same *ATXN7L3* transcript breakpoint has previously been identified in a patient with diffuse large B cell lymphoma (*GPATCH8::ATXN7L3*) [3], suggesting a shared driver function in different B-lymphoid malignancies. Both fusion partners were highly expressed across the entire cohort without significant

¹Medical Department II, Hematology and Oncology, University Medical Center Schleswig-Holstein, Kiel, Germany. ²University Cancer Center Schleswig-Holstein, University Medical Center Schleswig-Holstein, Kiel and Lübeck, Germany. ³Clinical Research Unit "CATCH-ALL" (KFO 5010/1), funded by the Deutsche Forschungsgemeinschaft (DFG, German Research Foundation), Bonn, Germany. ⁴Institute for Clinical Molecular Biology, Kiel University, Kiel, Germany. ⁵Institute of Human Genetics, University Medical Center Schleswig-Holstein, Kiel & Lübeck, Germany. ⁶DZHK (German Centre for Cardiovascular Research), Partner Site Hamburg/Lübeck/Kiel, 23538 Lübeck, Germany. ⁷Medical Systems Biology Group and Institute for Cardiogenetics, University of Lübeck, Lübeck, Germany. ⁸University Hospital Schleswig-Holstein, Campus Lübeck, Lübeck, Germany. ⁹Department of Hematology, Oncology and Tumor Immunology (Campus Benjamin Franklin), Charité-Universitätsmedizin Berlin, corporate member of Freie Universität Berlin and Humboldt-Universität zu Berlin, Berlin, Germany. ¹⁰Department of Medicine II, Hematology/Oncology, Goethe University Hospital, Frankfurt/M, Germany. ¹¹Department of Internal Medicine III, University Hospital Ulm, Ulm, Germany. ¹²Department of Hematology, Oncology and Clinical Immunology, University Hospital Düsseldorf, Düsseldorf, Germany. ¹³Department of Hematology and Oncology, University Hospital Göttingen, Göttingen, Germany. ¹⁴Medical Department V, Hospital Nürnberg, Paracelsus Medizinische Privatuniversität, Nürnberg, Germany. ¹⁵Medical Department Oncology and Hematology, University Medical Center Oldenburg, Oldenburg, Germany. ¹⁶Department of Medicine IV, Hematology/Oncology, Klinikum Bayreuth, Bayreuth, Germany. ¹⁷Comprehensive Cancer Center Erlangen-EMN (CCC ER-EMN), Erlangen, Germany. ✉email: Claudia.baldus@uksh.de

Received: 20 December 2021 Accepted: 23 March 2022

Published online: 9 April 2022



differences in the novel subtype (Supplementary Fig. S4), suggesting either gain-of-function or a dominant-negative effect of the gene fusion.

Both, UBTF and ATXN7L3 are global epigenetic regulators involved in transcriptional control. UBTF is an essential co-

activator of ribosomal RNA expression. Very recently, UBTF has been characterized as novel oncogene in acute myeloid leukemia (AML), where internal tandem duplications define a distinct molecular subtype with poor outcome and highest incidence in early adolescents [4, 5]. WGS and sanger sequencing ruled out

Fig. 1 *UBTF::ATXN7L3* gene fusion defines a BCP-ALL molecular subtype. Bone marrow or peripheral blood samples of $n = 568$ adult patients at first diagnosis of BCP-ALL with at least 20% blast infiltration were analyzed by transcriptome sequencing. Gene expression profiles of previously established definitions [1] were used to train a machine learning algorithm (Extreme Gradient Boosting) with feature selection (LASSO) to allocate samples to 15 established and 2 novel BCP-ALL subtypes. **A** Uniform manifold approximation and projection (UMAP) plot depicts distribution of molecular ALL subtypes based on expression of the top informative genes for subgroup allocation. **B** Unsupervised clustering of gene expression specific for the novel *UBTF::ATXN7L3* subgroup. Subtype-specific gene sets were identified by multi-comparison ANOVA using the variance stabilizing transformation for normalizing expression values. Genes had to be differentially expressed to at least 11 other subtypes with an FDR-corrected p value ≤ 0.01 (Supplementary Table S1,2). **C** Expression of selected *UBTF::ATXN7L3*-specific oncogenes is shown in comparison to other molecular subtypes with at least three samples. The complete list of Cosmic cancer gene census genes differentially expressed by multi-comparison ANOVA in *UBTF::ATXN7L3* ALL is shown in Supplementary Table S2. Expression of cancer-associated genes upregulated in *UBTF::ATXN7L3* in comparison to other molecular subtypes is shown in Supplementary Figure S6. **D** Subtype-specific driver fusions and the novel candidate driver gene fusion *UBTF::ATXN7L3* were called from RNA-Seq data (FusionCatcher) [15] Virtual karyotypes were obtained from whole-exome sequencing or SNP-Arrays (Illumina Infinium Global Screen array v3.0) to support classification of aneuploid subtypes. Subtype-specific hotspot driver mutations (eg. *PAX5*) were called from RNA-Seq data. Heatmap depicts probabilities for allocation of samples to the molecular subtypes (class probabilities) obtained by the gene expression-based machine learning classifier together with corresponding genomic driver events. * indicates one *UBTF::ATXN7L3* sample with 20% blast content, where the driver gene fusion was not called by FusionCatcher but was confirmed by break-point specific PCR and sanger sequencing (Supplementary Fig. S7B).

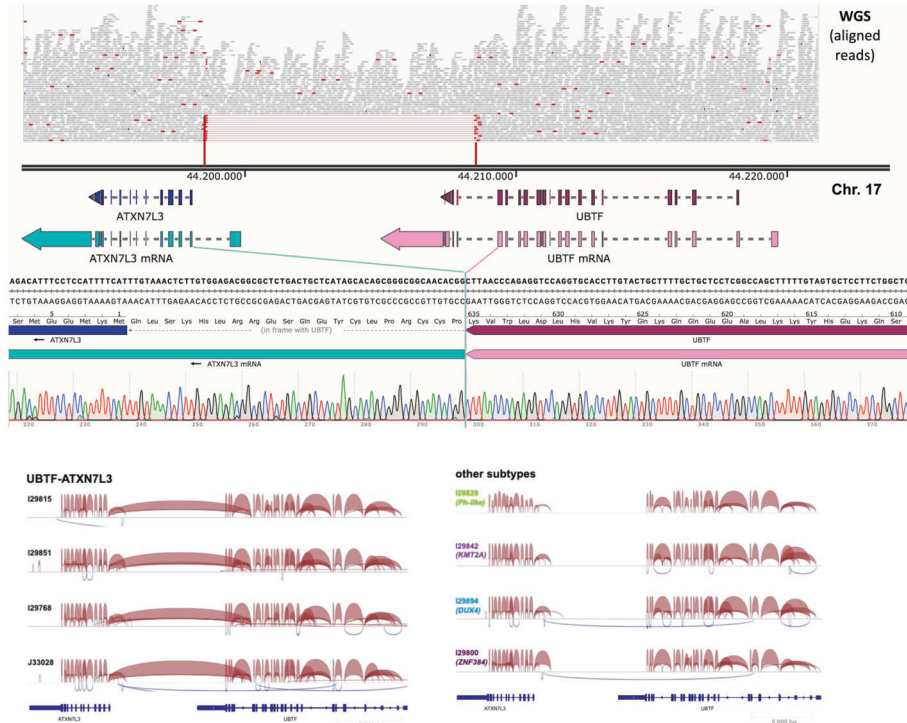
UBTF internal tandem duplications in *UBTF::ATXN7L3* patients (data not shown). *ATXN7L3* is a global gene expression co-activator through the SAGA complex. It is essential for activation of the SAGA histone deubiquitinase module (DUBm) through USP22, which is part of the 11-gene signature “Death-from-cancer” [6] defining poor outcomes across entities. The SAGA DUBm competes for *ATXN7L3*-binding with other deubiquitinases suggesting global changes in gene expression upon imbalances in *ATXN7L3*-substrate binding [7]. These findings align well with data on other molecular ALL subtypes driven by epigenetic perturbations [8, 9]. Analysis of subtype-specific gene expression by multi-comparison ANOVA revealed 332 genes with differential expression in *UBTF::ATXN7L3* ALL when compared to each other subtype (Fig. 1B; Supplementary Tables S1 and 2). These differentially expressed genes included upregulation of 18 cancer-associated genes (COSMIC Cancer gene census, Supplementary Table S3), one of which was *CDX2*, which has been used to define ‘*CDX2*-high’ ALL [2] (Fig. 1C). However, few samples from other subtypes also showed increased *CDX2* expression levels, limiting its applicability to identify this subtype. UBTF and *ATXN7L3* are global epigenetic regulators without described functional interactions with *CDX2*. *CDX2* is expressed in AML [10] and ALL [11], independently of the driver subtype. Conditional *Cdx2* overexpression in hematopoietic progenitors resulted in myelodysplasia but required acquisition of secondary aberrations for leukemic transformation [12], suggesting a cooperative function during leukemogenesis. Although *UBTF::ATXN7L3*-specific gene expression showed little overlap with published *CDX2* overexpression models (Supplementary Fig. S5A), we identified a functional module relating *CDX2* to *HOXA9* and *MEIS1* overexpression in *UBTF::ATXN7L3* ALL, in line with similar findings in AML [13] (Supplementary Figure S5B,C). *HOXA9/MEIS1* are essential co-factors for KMT2A-driven leukemogenesis [9], making it possible that a *CDX2-HOXA9/MEIS1* axis exerts a similar leukemia promoting role in *UBTF::ATXN7L3* ALL. Further oncogenes related to hematologic malignancies were also upregulated in *UBTF::ATXN7L3* patients (Fig. 1C, Supplementary Figure S6), including *NTRK3* which might represent a therapeutic target for specific inhibitors (e.g. larotrectinib, entrectinib). To evaluate additional genomic driver aberrations, we performed WES ($n = 7$) and/or SNP-array analyses ($n = 6$) showing a described enrichment of chromosome 1q gains [2] ($n = 5/7$) and heterogeneous single chromosome aberrations. However, no subtype-specific recurrent driver events were identified (Supplementary Fig. S7A), supporting the functional relevance of *UBTF::ATXN7L3* as recurrent hallmark of this subtype. *UBTF::ATXN7L3* ALL was enriched for pro-B immunophenotypes ($n = 5/12$, 42% vs. $n = 70/530$, 13%; $p = 0.016$) and occurred predominantly in female

patients ($n = 10/12$, 83% vs. 237/534, 44%; $p = 0.008$) and patients of advanced age (median: 48.5 years vs. 38 years; $p = 0.05$).

Outcome evaluable *UBTF::ATXN7L3* patients ($n = 11/12$; Fig. 2B) received treatments on pediatric inspired GMALL protocols. Risk stratification identified 6 patients as high-risk due to pro-B immunophenotype ($n = 4$) or late response ($n = 2$). One patient died during induction therapy and another patient failed to achieve hematologic CR after consolidation I (overall cytologic CR rate: 82%). Only $n = 3/10$ patients cleared MRD after consolidation I (cytologic and molecular CR) compared to $n = 271/402$ (67%; $p = 0.019$; Fig. 2C) in the remaining cohort. Two out of these three good responders remained in molecular CR after conventional chemotherapy including allogeneic stem cell transplantation (HSCT) due to high-risk criteria. One patient relapsed after discontinuation of standard chemotherapy due to poor performance status and achieved a second molecular CR after inotuzumab ozogamizine. Patients with intermediate MRD response (positive MRD $< 10^{-4}$ or below quantifiable range, $n = 3$) experienced molecular relapses on standard therapy, received Blinatumomab followed by HSCT and remained in long-term remission ($n = 2/3$) or achieved sustained CR on standard therapy ($n = 1/3$). Among the remaining poor responders ($n = 4$), one cytologic non-responder achieved MRD-negativity after Blinatumomab, received HSCT and died due to transplant-related complications. Two patients received Blinatumomab, achieved a molecular CR, proceeded to HSCT, and remained in long-term remission. The fourth patient received HSCT without Blinatumomab, relapsed, and achieved intermediate MRD after 2nd HSCT. Together, we observed a median overall survival probability of *UBTF::ATXN7L3* patients of 80% ($\pm 12\%$) compared to 73% ($\pm 2\%$; $p = 0.07$; Fig. 2D) in the remaining cohort, which is comparable to the ongoing GMALL08/2013 study [14]. Yasuda et al [2] reported markedly lower survival rates (pOS: 26.7%, (4.8–56.3)) in ‘*CDX2*-high’ patients treated in historical cohorts without MRD-based risk stratification. Together, these data suggest that *UBTF::ATXN7L3* ALL represents a less chemo-sensitive disease subtype, which can be successfully salvaged by current MRD-based concepts incorporating immunotherapies and stem cell transplantation [14].

Other subtypes with poor MRD response in our cohort included ZNF384 (48.2% MRD negative after consolidation I; $p = 0.056$), Ph-like ALL (54.0% MRD negative, $p = 0.003$) and KMT2A (55.8% MRD negative, $p = 0.127$), whereas high hyperdiploid (90.9% MRD negative, $p = 0.01$) and TCF3::PBX1 (94.1% MRD negative, $p = 0.016$) subtypes showed favorable MRD responses. This heterogeneity and recently published differences in treatment outcomes of ALL subtypes when treated with or without MRD-based risk-stratification highlight the importance of evaluating the clinical

A

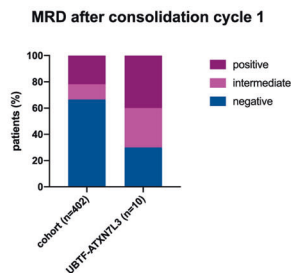


B

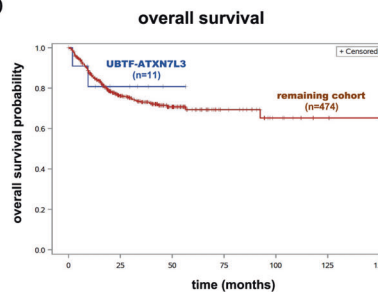
patient	age (years)	sex	immuno-phenotype	initial WBC count (cells / μ L)	initial risk stratification	cytologic remission after consolidation I	minimal residual disease after consolidation I	therapy course after consolidation I	outcome
21ORD12106	55	female	common	5.050	SR	CR	negative	standard chemotherapy	molecular CR
I29863	54	female	pro-B	3.400	HR	CR	negative	standard chemotherapy, discontinued due to poor performance status, relapse, inotuzumab	molecular CR
J33028	51	female	common	5.100	SR, re-stratified HR (PR after induction I)	CR	negative	HSCT	molecular CR
J32981	54	female	pro-B	4.800	HR	not reached	not reached	death in induction cycle II	induction death
I29815	40	female	common	11.300	SR	CR	intermediate (pos$3 \times 10^{-5}>1 \times 10^{-6}$)	standard chemotherapy	molecular CR
21ORD11998	40	male	common	7.100	SR	CR	intermediate (pos5×10^{-5})	standard chemotherapy, molecular relapse, molecular CR after blinatumomab, HSCT	molecular CR
21ORD12022	55	female	common	6.630	SR	CR	intermediate (pos$5 \times 10^{-5}>1 \times 10^{-6}$)	standard chemotherapy, molecular relapse, molecular CR after blinatumomab, HSCT	molecular CR
I29768	39	female	common	1.800	SR	failure	positive (cytologic failure)	molecular CR after blinatumomab, HSCT	transplant-related death
I29851	46	female	common	13.810	SR, re-stratified HR (PR after induction I)	CR	positive (2×10^{-3})	molecular CR after blinatumomab, HSCT	molecular CR
J32993	31	female	pro-B	3.470	HR	CR	positive (4×10^{-4})	molecular CR after blinatumomab, HSCT	molecular CR
BERLINML3417	30	male	pro-B	7.320	HR	CR	positive (3×10^{-3})	HSCT in molecular failure, relapse, 2nd HSCT, MRD positive < quantitative range	lost to follow-up

Abbreviations: WBC, white blood cell; SR, standard risk; HR, high risk; CR, complete remission, PR, partial remission; HSCT, hematopoietic stem cell transplantation

C



D



course of novel molecular subgroups in the context of current treatment strategies.

Yasuda et al [2]. described a second novel BCP-ALL subtype defined by *IDH1/2* hotspot mutations (1.9% of cohort). We screened RNA-Seq data of all remaining ‘unassigned’ samples of

our cohort ($n = 22$) for the described gene expression signature or *IDH1/2* mutations and identified one patient harboring *IDH2* p. R140Q, which was confirmed by PCR on gDNA level, contributing to the heterogeneous frequency distribution of molecular subtypes in different BCP-ALL cohorts.

Fig. 2 UBTF::ATXN7L3 ALL patients experience poor responses to conventional chemotherapy and successful salvage by MRD-stratified treatment intensification including immunotherapies. A The structure of *UBTF::ATXN7L3* fusion is shown. Above: whole-genome sequencing read alignment from one representative sample (I29815) with reads depicted as pairs and red highlighting insert lengths above the 99.5 percentile of all reads; middle: NCBI reference sequence of 17q21.31 (chr17:44,191,805–44,221,804); below: sanger sequence of a break-point specific PCR on cDNA and sashimi plots depicting junction reads from RNA-Seq data of representative *UBTF::ATXN7L3* patients and representative patients from other subtypes. **B** Basic clinical characteristics, treatment courses and outcome of *UBTF::ATXN7L3* patients are shown. **C** Minimal residual disease (MRD) was measured by clone-specific real-time quantitative PCR of immune gene rearrangements after consolidation cycle I. Negative: MRD negative with sensitivity of at least 10^{-4} , positive: MRD above 10^{-4} also including cytologic non-response, intermediate: MRD positive $< 10^{-4}$ or below quantifiable range. **D** Overall survival analysis of *UBTF::ATXN7L3* patients compared to the remaining cohort.

Our data identify *UBTF::ATXN7L3* resulting from a 17q21.31 variant as novel subgroup defining candidate driver fusion for the recently described 'CDX2-high ALL' subtype. Poor MRD response indicates reduced chemosensitivity in these patients. Our data suggest MRD-based treatment intensification using salvage immunotherapies and allogenic stem cell transplantation as a promising strategy to rescue this high-risk phenotype.

REFERENCES

- Bastian L, Schroeder MP, Eckert C, Schlee C, Sanchez JO, Kämpf S, et al. PAX5 biallelic genomic alterations define a novel subgroup of B-cell precursor acute lymphoblastic leukemia. *Leukemia*. 2019;33:1895–909.
- Yasuda T, Sanada M, Kawazu M, Kojima S, Tsuzuki S, Ueno H et al. Two novel high-risk adult B-cell acute lymphoblastic leukemia subtypes with high expression of *CDX2* and *IDH1/2* mutations. *Blood*. 2021; blood.2021011921.
- Gao Q, Liang W-W, Foltz SM, Mutharasu G, Jayasinghe RG, Cao S, et al. Driver fusions and their implications in the development and treatment of human cancers. *Cell Rep*. 2018;23:227–e3.
- Stratmann S, Yones SA, Mayrhofer M, Norgren N, Skaftason A, Sun J, et al. Genomic characterization of relapsed acute myeloid leukemia reveals novel putative therapeutic targets. *Blood Adv*. 2021;5:900–12.
- Umeda M, Ma J, Huang BJ, Hagiwara K, Westover T, Abdelhamed S et al. Integrated genomic analysis identifies UBTF tandem duplications as a recurrent lesion in pediatric acute myeloid leukemia. *Blood Cancer Discov* 2022: blood-candisc.BCD-21-0160-A.2021.
- Glinsky GV, Berezovska O, Glinskii AB. Microarray analysis identifies a death-from-cancer signature predicting therapy failure in patients with multiple types of cancer. *J Clin Investig*. 2005;115:1503–21.
- Atanassov BS, Mohan RD, Lan X, Kuang X, Lu Y, Lin K, et al. *ATXN7L3* and *ENY2* coordinate activity of multiple H2B deubiquitinases important for cellular proliferation and tumor growth. *Mol Cell*. 2016;62:558–71.
- Huang Y, Mouttet B, Warnatz H-J, Risch T, Rietmann F, Frommelt F, et al. The leukemogenic TCF3-HLF complex rewires enhancers driving cellular identity and self-renewal conferring EP300 vulnerability. *Cancer Cell*. 2019;36:630–644.e9.
- Ayton PM, Cleary ML. Transformation of myeloid progenitors by MLL oncoproteins is dependent on *Hoxa7* and *Hoxa9*. *Genes Dev*. 2003;17:2298–307.
- Scholl C, Bansal D, Döhner K, Eiwien K, Huntly BJP, Lee BH, et al. The homeobox gene *CDX2* is aberrantly expressed in most cases of acute myeloid leukemia and promotes leukemogenesis. *J Clin Investig*. 2007;117:1037–48.
- Thoene S, Rawat VPS, Heilmeier B, Hoster E, Metzeler KH, Herold T, et al. The homeobox gene *CDX2* is aberrantly expressed and associated with an inferior prognosis in patients with acute lymphoblastic leukemia. *Leukemia*. 2009;23:649–55.
- Vu T, Straube J, Porter AH, Bywater M, Song A, Ling V, et al. Hematopoietic stem and progenitor cell-restricted *Cdx2* expression induces transformation to myelodysplasia and acute leukemia. *Nat Commun*. 2020;11:3021.
- Rawat VPS, Thoene S, Naidu VM, Arseni N, Heilmeier B, Metzeler K, et al. Overexpression of *CDX2* perturbs *HOX* gene expression in murine progenitors depending on its N-terminal domain and is closely correlated with deregulated *HOX* gene expression in human acute myeloid leukemia. *Blood*. 2008;111:309–19.
- Goekbuget N, Stelljes M, Viardot A, Nachtkamp K, Steffen B, Schneller F, et al. First results of the risk-adapted, MRD-stratified GMALL trial 08/2013 in 705 adults with newly diagnosed acute lymphoblastic leukemia/lymphoma (ALL/LBL). *Blood*. 2021;138:362–362.
- Nicorici D, Satalan M, Edgren H, Kangaspekka S, Murumagi A, Kallioniemi O, et al. FusionCatcher - a tool for finding somatic fusion genes in paired-end RNA-sequencing data. 2014. <https://www.biorxiv.org/content/10.1101/011650v1>.

ACKNOWLEDGEMENTS

This study was in part funded by funded by the Deutsche Forschungsgemeinschaft (DFG, German Research Foundation) – project number 444949889 (KFO 5010/1 Clinical Research Unit 'CATCH ALL' to LB, AH, MPH, MN, MBr, and CDB), Deutsche Jose Carreras Leukämie Stiftung (DJCLS 01R/2016 to LB and CDB).

AUTHOR CONTRIBUTIONS

LB, MBr and CDB designed the study; LB, AMH, TB, SH, JK, and MN processed, analyzed, and interpreted high-throughput sequencing data; MBu performed and analyzed experiments; SF, MW, AF, IN, MS, MPH performed high-throughput sequencing and processed data; LB, AMH, TB, SH, and NG performed statistical analyses; SS, BS, AV, KD, MK, GW, KW, AR, AK, HT, HT, MBr and NG contributed and interpreted data; LB, NG, and MBr supervised the project; LB, AMH, TB and CDB drafted the first version of the manuscript; and all authors revised and approved the final version of the manuscript.

FUNDING

Open Access funding enabled and organized by Projekt DEAL.

COMPETING INTERESTS

MBr received personal fees from Incyte (advisory board) and Roche Pharma AG, financial support for reference diagnostics from Affimed and Regeneron, grants and personal fees from Amgen (advisory board, speakers bureau, travel support), and personal fees from Janssen (speakers bureau), all outside the submitted work. The remaining authors declare no competing financial interests. None of the remaining authors has a relevant conflict of interest.

ADDITIONAL INFORMATION

Supplementary information The online version contains supplementary material available at <https://doi.org/10.1038/s41375-022-01557-6>.

Correspondence and requests for materials should be addressed to Claudia D. Baldus.

Reprints and permission information is available at <http://www.nature.com/reprints>

Publisher's note Springer Nature remains neutral with regard to jurisdictional claims in published maps and institutional affiliations.



Open Access This article is licensed under a Creative Commons Attribution 4.0 International License, which permits use, sharing, adaptation, distribution and reproduction in any medium or format, as long as you give appropriate credit to the original author(s) and the source, provide a link to the Creative Commons licence, and indicate if changes were made. The images or other third party material in this article are included in the article's Creative Commons licence, unless indicated otherwise in a credit line to the material. If material is not included in the article's Creative Commons licence and your intended use is not permitted by statutory regulation or exceeds the permitted use, you will need to obtain permission directly from the copyright holder. To view a copy of this licence, visit <http://creativecommons.org/licenses/by/4.0/>.

© The Author(s) 2022